

# Self-Supervised Anomaly Detection by Self-Distillation and Negative Sampling

Nima Rafiee<sup>1</sup>    Rahil Gholamipoorfard<sup>1</sup>    Nikolas Adaloglou<sup>1</sup>    Simon Jaxy<sup>1</sup>  
Julius Ramakers<sup>1</sup>  
Markus Kollmann<sup>1,2</sup>

<sup>1</sup>Department of Computer Science, Heinrich Heine University, D-40225 Dusseldorf

<sup>2</sup>Department of Biology, Heinrich Heine University, D-40225 Dusseldorf;

{rafiee, rahil.gholamipoorfard, nikolaos.adaloglou, simon.jaxy, ramakers, kollmann}@hhu.de

## Abstract

*Detecting whether examples belong to a given in-distribution or are Out-Of-Distribution (OOD) requires identifying features specific to the in-distribution. In the absence of labels, these features can be learned by self-supervised techniques under the generic assumption that the most abstract features are those which are statistically most over-represented in comparison to other distributions from the same domain. In this work, we show that self-distillation of the in-distribution training set together with contrasting against negative examples derived from shifting transformation of auxiliary data strongly improves OOD detection. We find that this improvement depends on how the negative samples are generated. In particular, we observe that by leveraging negative samples, which keep the statistics of low-level features while changing the high-level semantics, higher average detection performance is obtained. Furthermore, good negative sampling strategies can be identified from the sensitivity of the OOD detection score. The efficiency of our approach is demonstrated across a diverse range of OOD detection problems, setting new benchmarks for unsupervised OOD detection in the visual domain.*

## 1. Introduction

OOD detection or anomaly detection is the problem of deciding whether a given test sample is drawn from the same in-distribution as a given training set or belongs to an alternative distribution. Many real-world applications require highly accurate OOD detection for secure deployment, such as in medical diagnosis. Despite the advances in deep learning, neural network estimators can generate systematic errors for test examples that are far from the train-

ing set [37]. For example, it has been shown that Deep Neural Networks (DNNs) with ReLU activation functions can make false predictions for OOD samples with arbitrarily high confidence [19].

A major challenge in OOD detection is the case where the features of outlier examples are statistically close to the features of in-distribution examples, which is frequently the case for natural images. In particular, it has been shown that deep density estimators like Variational Autoencoders (VAEs) [25], PixelCNNs [48], and normalising flow models [40] can on average assign higher likelihood to OOD examples than to examples from the in-distribution [34]. This surprising finding can be partially attributed to an inductive bias from upweighting local pixel correlations as a consequence of using convolutional neural networks.

A challenging scenario of anomaly detection is near OOD detection [51], where the OOD distribution samples are statistically very similar to the in-distribution. A particular challenging OOD detection task is given by CIFAR100 [27] as in-distribution and CIFAR10 [27] as OOD, where the larger number of classes in CIFAR100 make it harder to identify features that are specific for the in-distribution. Another aspect is that OOD detection becomes more challenging if there exists a substantial class overlap between the in-distribution and the out-distribution. For instance, CIFAR10 and STL10 [10] share 7 out of 10 of their classes. Finally, there are cases where the in and out distributions are not closely related, which we refer to as far OOD.

State-Of-The-Art (SOTA) performance has been obtained for the CIFAR100/CIFAR10 near OOD detection task, using pretrained classification models using ImageNet-21K [14]. However, as CIFAR100 and CIFAR10 share many of their classes with ImageNet but the classes among themselves are mutually exclusive, the pretrained model effectively solves the OOD detection problem for this special case. The advantage of using pretrained models as OOD detectors drops if there is no class overlap with

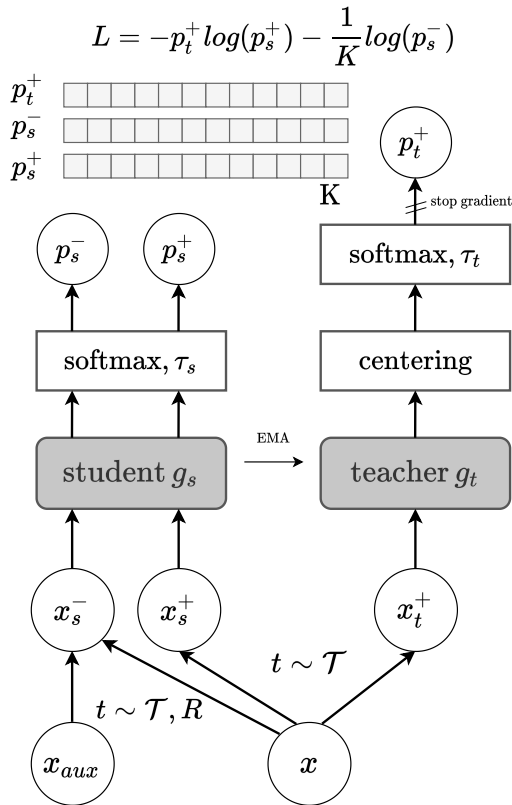


Figure 1. An overview of the proposed contrastive self-distillation framework, consisting of student and teacher networks,  $g_s$  and  $g_t$ , that map two random transformations of the same image,  $x_s^+ \sim \mathcal{T}(x)$  and  $x_t^+ \sim \mathcal{T}(x)$  to the same class. Negative views,  $x^-$ , arise from first applying a shifting transformation  $R$ , such as random rotation, followed by  $\mathcal{T}$  to either an in-distribution image  $x$  or an auxiliary image  $x_{aux}$ .

the OOD test set, such as for SVHN [14]. Moreover, such massive annotated datasets with sufficient class overlap are rarely available, while unlabeled data are often widely accessible. It has also been argued that the image-level supervision may reduce the rich visual signal contained in an image to a single concept [4, 41].

To overcome these limitations, a plethora of self-supervised pretext tasks have been proposed that provide a richer learning signal that enables abstract feature learning [3, 5, 18]. These advancements in self-supervised learning have shown remarkable results on unsupervised anomaly detection [43, 46, 51] by solely relying on the in-distribution data.

More recently, it has been suggested to include dataset-specific augmentations that shift the in-distribution – so-called negative samples. The core idea behind using shifting transformations is to concentrate the learned representation

in feature space. This can result in a more conservative decision boundary for the in-distribution [22]. However, in-distribution shifting requires dataset-specific prior knowledge [33]. Therefore, a bad choice of augmentations may result in rejecting the in-distribution test samples, which reduces the OOD detection performance.

On the model side, Vision Transformers (ViT) [12] have been established in many computer vision tasks, such as image classification, and semantic segmentation [54]. ViTs are capable of capturing long-range correlations, which is crucial for learning high-level semantics. Specifically, robust representations can be generated from ViTs by formulating a label-free self-distillation task (DINO [4]). The DINO objective aims to map different augmentations of the same image to the same “soft” class. The learned features of DINO have been shown to contain explicit information about the image semantics.

In this paper, we propose an improved version of the DINO [4] framework in the context of OOD detection. The main contributions of this work are summarized as follows:

- We propose a general methodology that leverages unlabelled data for OOD detection.
- We provide strategies on how negative samples can be generated in a systematic way by using the score for rejecting in-distribution test examples as OOD as a sensitivity measure.
- We introduce an auxiliary loss that encourages negative samples to be uniformly assigned to the existing in-distribution soft-classes.
- Finally, we show that the proposed framework does not only improve OOD detection performance but also improves representation learning for the in-distribution, as measured by the K-Nearest Neighbour (K-NN) accuracy.

## 2. Related works

**Supervised OOD detection methods.** In-distribution classification accuracy is highly correlated with OOD performance [15]. This motivated supervised OOD detection approaches to learn representations from classification networks. This can be achieved by directly training a classifier on the in-distribution or by pretraining on a larger dataset. Hendrycks et al. [20] used Maximum Softmax Probabilities (MSP) to discriminate between OOD and in-distribution samples. In-distribution classifiers have been improved by introducing additional training tricks and strategies. In [29], the authors demonstrated that the MSP performance can be increased by using a temperature parameter. In the same direction, various works focused on forming alternative loss functions [28, 50] or auxiliary objectives [11, 23, 32] to learn

a robust representation from the in-distribution classification.

Fine-tuning pretrained transformers [49] has shown promising OOD scores. Hendrycks et al. [21] showed that transformers are more robust to detecting outliers when pretrained on larger and more diverse natural language datasets. Similarly, in computer vision, Koner et al. [26] leveraged the contextualization capabilities of pretrained ViTs by exploiting the global image context. Fort et al. [15] fine-tuned ViTs for anomaly detection that were pretrained on ImageNet-21K. While fine-tuning on the in-distribution, they further highlighted the few-shot OOD performance of such models. These kinds of large-scale pretrained models heavily rely on the classes of the pretraining dataset, which often include classes from both the in and out distribution. Hence, supervised pretraining can form a good boundary for OOD detection. However, supervised pretraining imposes two limitations for anomaly detection: a) the pretraining dataset should share labels with both distributions (in and out), and b) impeded OOD performance is observed when the distributions have overlapping classes.

Several recently developed methods [28, 52, 56] used annotated data to learn an intermediate representation on which a density distribution can be fitted to compute the likelihood of OOD examples. In [45], the authors used multiple regression functions to build a robust classifier in order to identify OOD inputs, while in [31] the authors used metric learning to learn an embedding where samples from the same in-distribution class form clusters. Representations can be further enhanced by combining image-supervision with contrastive learning [52]. Supervised contrastive learning [8, 24] has also been successfully applied for anomaly detection. In [6], the authors showed an alternative way of leveraging labels by creating class-conditional masks for contrastive learning. This task-specific variant of supervised contrastive learning shaped more clear boundaries between in-distribution classes, which is more befitted for OOD detection.

Mohseni et al. [33] recently presented a 2-step method that initially learns how to weight the in-distribution transformations based on a supervised objective. Then, the selected shifting transformations are applied in a self-supervised setup for OOD detection. Still, human-level supervision is required to learn the best shifting transformations for each training dataset. In *Geometric* [23], Hendrycks et al. defined a self-supervised task to predict geometric transformations to improve the robustness and uncertainty of deep learning models. They further improved their self-supervised technique with supervision through outlier exposure, encouraging the network to uniformly distribute OOD samples among in-distribution classes.

**Unsupervised OOD detection methods.** Existing label-free OOD detection approaches can be separated in: a)

density-based [35, 39, 44], b) reconstruction-based [38, 58], and c) self-supervised learning [16, 23] ones. Density-based methods aim to fit a probability distribution such as Gaussian on the training data and then use it for OOD detection. Reconstruction-based methods assume that the network would generalize less for unseen OOD samples. Deep generative models like VAEs were widely used for OOD detection [1], motivated by the idea that VAEs [25] cannot reconstruct OOD samples fairly well. Meanwhile, recent studies [34] revealed that probabilistic generative models can fail to distinguish between training data and OOD inputs. To address this issue, some efficient OOD scores were proposed based on likelihood [35, 39, 53]. Schirrmeyer et al. [42] leveraged the hierarchical view of distributions to propose a likelihood-based anomaly detection method. More precisely, they train two identical generative architectures, one trained on the in-distribution and one on a more general distribution.

Self-supervised methods have recently shown that adopting pretext tasks results in learning general data representations [13] for OOD detection. Choi et al. [7] used blurred data as adversarial examples to discriminate the training data from their blurred versions. In [16], a multi-class image classifier is trained to discriminate geometric transformations. The OOD images were then detected, by comparing the softmax probabilities of their transformed instances against train data. To extend the aforementioned method to non-imaging data, Bergman et al. [2] extended the set of transformations to affine transformations.

In *CSI* [46], Tack et al. leverage shifting data transformations in contrastive learning for OOD detection, combined with an auxiliary task that predicts which shifting transformation was applied to a given input. They also demonstrated how an OOD score function can utilize contrastive representations. In *SSD* [43], the authors further improved contrastive self-supervised training by developing a cluster-conditioned OOD detection method in the feature space.

**Outlier Exposure (OE).** OE leverages auxiliary data that are utterly disjoint from the OOD data [22]. Furthermore, OE assumes that the provided auxiliary samples are always OOD. To guarantee this, human supervision is necessary to remove the overlap between auxiliary and in-distribution. OE has been successfully applied to training classifiers, by enforcing the auxiliary samples to be equally distributed among the in-distribution classes. Inspired by [22], we attempt to teach the network better representations for OOD detection by incorporating auxiliary data into a self-distillation soft-labeling framework.

Finally, since the proposed method does not require labels, there is no information on whether the in-distribution data are meaningfully similar to the auxiliary ones. In this aspect, this work is different from OE, as it only requires the in-distribution to be sufficiently statistically underrepre-

sented. To ensure the latter, an additional transformation  $R$  is applied on the auxiliary data.

### 3. Proposed Method

#### 3.1. The vanilla DINO framework

The DINO framework uses two identical networks  $g_s = g(x|\theta_s)$  and  $g_t = g(x|\theta_t)$  called student and teacher, which differ by their sets of parameters  $\theta_s$  and  $\theta_t$ , respectively. For each transformed input image  $x$ , both networks produce  $K$ -dimensional output vectors, where  $K$  is the number of soft-classes. Both outputs enter a temperature-scaled softmax functions  $p_t = \text{softmax}(g_t, \tau_t)$  and  $p_s = \text{softmax}(g_s, \tau_s)$  defined by:

$$p^i(x) = \frac{\exp(g^i(x)/\tau)}{\sum_{k=1}^K \exp(g^k(x)/\tau)}, \quad (1)$$

where  $p^i(x)$  is the probability of  $x$  falling in soft-class  $i$  and  $\tau_s, \tau_t$  are the student and teacher temperatures. In contrast to knowledge distillation methods, the teacher is built from previous training iterations of the student network. To do so, the gradients are back-propagated only through the student network and the teacher parameters are updated with the Exponential Moving Average (EMA) of the student parameters

$$\theta_t \leftarrow m\theta_t + (1 - m)\theta_s, \quad (2)$$

where  $0 \leq m \leq 1$  is a momentum parameter. For  $\tau_t < \tau_s$ , the training objective is given by the cross entropy loss for two non-identical transformations  $x'', x'$  of an image  $x$  drawn from the in-distribution training set  $\mathcal{D}_{train}^{in}$

$$\mathcal{L}_{pos} = - \sum_{x'' \in G} \sum_{\substack{x' \in V \\ x' \neq x''}} p_t(x'') \log(p_s(x')). \quad (3)$$

Additionally, DINO uses the multi-crop strategy [3], wherein  $M$  global views  $G = \{x_1^g, \dots, x_M^g\}$  and  $N$  local views,  $L = \{x_1^l, \dots, x_N^l\}$ , are generated based on a set of transformations  $\mathcal{T}$ , e.g. crop and resize, horizontal flip, Gaussian blur, and color jitter. Global views are crops that occupy a larger region of the image (e.g.  $\geq 40\%$ ) while local views cover small parts of the image (e.g.  $\leq 40\%$ ). All  $V = G \cup L$  views are passed through the student network, while the teacher has only access to the global views such that local-to-global correspondences are enforced. The trained teacher network is used for evaluation.

#### 3.2. Negative samples

The learning objective (Eq. (3)) assigns two transformed views of an image to the same soft-class. The applied transformations  $\mathcal{T}$  are chosen to be sufficiently strong and diverse, such that the generated images generalise well over

the training set but keep the semantics of the image they were derived from. The transformations are designed to learn higher-level features such as labels that represent semantic information and avoid learning lower-level features, such as edges or the color statistics over pixels [5]. The quality of the learned representation can be quantified by evaluating the K-NN accuracy for an in-distribution test set  $\mathcal{D}_{test}^{in}$ , using as higher-level feature vector an activity map of the network near the last layer. For OOD detection, the feature vector representation should be enriched by in-distribution-specific features and depleted by features that frequently appear in other distributions from the same domain. This can be achieved by designing a negative distribution  $\mathcal{D}_{neg}$  that keeps most of the low-level features of the in-distribution but changes the high-level semantics.

For example, a negative distribution for natural images can be realised by additionally rotating in-distribution images or images from a related auxiliary distribution by  $r \sim R = \mathcal{U}(\{90^\circ, 180^\circ, 270^\circ\})$ , where  $\mathcal{U}$  is the uniform distribution. It has been shown that using rotation as an additional positive transformation degrades the performance in the contrastive learning setup, where the objective is to maximize the mutual information between positive examples [5]. Motivated by this, authors in [46] report a performance gain for OOD detection by using rotation to generate negative examples.

#### 3.3. Auxiliary objective

In addition to the self-distillation objective Eq. (3) we define an auxiliary task to encourage the student to have a uniform softmax response for negative examples. This task can be realised by a similar objective as Eq. (3) but with changed temperature  $\tau_t \rightarrow \infty$  and transformations  $\mathcal{T}$  applied to examples  $x$  from the negative set  $\mathcal{D}_{neg}$ , defined as:

$$\mathcal{L}_{neg} = -\frac{1}{K} \sum_{x' \in V} \log p_s(x'). \quad (4)$$

The total loss of our proposed method is defined by a linear combination of the two objectives

$$\mathcal{L}_{total} = \mathcal{L}_{pos} + \lambda \mathcal{L}_{neg}, \quad (5)$$

where  $\lambda > 0$  is a balancing hyperparameter.

### 4. Experiments

The proposed method is based on the vanilla DINO [4] implementation<sup>1</sup>. Unless otherwise specified, we use ViT-Small (ViT-S) with a patch size of 16. We use  $N = 8$  local views for both positives and negatives, but two global positive views and one global negative view. Global views are resized to  $256 \times 256$  while local views to  $128 \times 128$ .

<sup>1</sup><https://github.com/facebookresearch/dino>

Table 1. AUROC scores for OOD detection without label supervision.

|                            |                            | OOD Detection AUROC (%) |          |              |                       |              |              |
|----------------------------|----------------------------|-------------------------|----------|--------------|-----------------------|--------------|--------------|
| $\mathcal{D}_{train}^{in}$ | $\mathcal{D}_{test}^{out}$ | Geometric* [23]         | SSD [43] | CSI [46]     | MTL <sup>†</sup> [33] | Ours         |              |
|                            |                            |                         |          |              |                       | Rot.<br>ImgN | Combined     |
| CIFAR10                    | CIFAR100                   | 91.91                   | 90.63    | 89.20        | 93.24                 | 92.51        | <b>94.20</b> |
|                            | SVHN                       | 97.96                   | 99.62    | 99.80        | <b>99.92</b>          | 99.69        | <b>99.92</b> |
|                            | ImageNet30                 | –                       | 90.20    | 87.92        | –                     | <b>94.16</b> | 93.40        |
|                            | TinyImageNet               | 92.06                   | 92.25    | 92.44        | 92.99                 | <b>96.28</b> | 95.02        |
|                            | LSUN                       | 93.57                   | 96.51    | 91.60        | 95.03                 | <b>98.08</b> | 97.52        |
|                            | STL10                      | –                       | 70.28    | 64.25        | –                     | <b>77.29</b> | 74.34        |
|                            | Places365                  | 92.57                   | 95.21    | 90.18        | 93.72                 | <b>97.14</b> | 96.01        |
|                            | Texture                    | 96.25                   | 97.61    | 98.96        | –                     | <b>99.16</b> | 98.69        |
| CIFAR100                   | CIFAR10                    | 74.73                   | 69.60    | 58.87        | <b>79.25</b>          | 69.96        | 67.63        |
|                            | SVHN                       | 83.62                   | 94.90    | 96.44        | 87.11                 | 96.00        | <b>97.17</b> |
|                            | ImageNet30                 | –                       | 75.53    | 71.82        | –                     | <b>84.82</b> | 75.36        |
|                            | TinyImagenet               | 77.56                   | 79.52    | 79.28        | 80.66                 | <b>81.41</b> | 79.75        |
|                            | LSUN                       | 71.86                   | 79.50    | 61.83        | 74.32                 | <b>85.03</b> | 74.55        |
|                            | STL10                      | –                       | 72.76    | 64.26        | –                     | <b>79.96</b> | 71.70        |
|                            | Places365                  | 74.57                   | 79.60    | 65.48        | 77.87                 | <b>81.67</b> | 72.79        |
|                            | Texture                    | 82.39                   | 82.90    | <b>87.47</b> | –                     | 80.65        | 77.33        |

\* Requires labels for the supervised training loss. Results reported from [33].

† Requires labels to select the optimal transformations.

The temperatures are set to  $\tau_t = 0.01$  and  $\tau_s = 0.1$ . In each epoch, we linearly decrease  $\tau_t$  starting from 0.055 for CIFAR10 and from 0.050 for CIFAR100 to 0.01 during training. We set  $\lambda$  to 1 for all our experiments, and  $K = 4096$ .

We use the Adamw optimizer [30] with an effective batch size of 256. The learning rate  $lr$  follows the linear scaling rule of  $lr = lr_{base} \times \text{batchsize} / 256$ , where  $lr_{base} = 0.004$ . All models are trained for 500 epochs. Experiments were conducted using 4 NVIDIA-A100 GPUs with 40GB of memory. The image augmentation pipeline  $\mathcal{T}$  is based on [4, 17]. Finally, weight decay and learning rate are scaled with a cosine scheduler.

#### 4.1. Datasets and negative sample variants

We evaluate our method on CIFAR10 and CIFAR100 as in-distribution data. For auxiliary datasets, we use ImageNet [41] and Debaised 300K Tiny Images (DTI) [22]. The latter is a subset with 300K images from [47], where images belong to CIFAR10, CIFAR100, Places365 [57], and LSUN [55] classes are removed. To avoid shortcut learning (due to different image resolutions), we resize the auxiliary data to the size of the in-distribution data before applying any augmentation. For OOD detection, we consider common benchmark datasets, such as SVHN [36], Places365, Texture [9] and STL10. The following cases are considered

for generating negative samples:

- DINO: no negatives are included ( $\lambda = 0$ ).
- ImgN: samples from ImageNet.
- DTI: samples from Debaised Tiny Images.
- Rot.: samples are randomly rotated by  $r \sim R = \mathcal{U}(\{90^\circ, 180^\circ, 270^\circ\})$ .
- Rot.360: samples are randomly rotated between  $0^\circ$  and  $360^\circ$  in  $90^\circ$  steps.
- Perm- $N$ : randomly permutes each part of the evenly partitioned image in  $N$  patches.
- Pix. Perm: randomly shuffles all the pixels in the image.
- Rot. In-Dist: a random rotation  $r \sim R$  is applied to the in-distribution data.
- Combined: both samples from Rot. In-Dist and Rot. ImageNet are used.

#### 4.2. Evaluation protocol for OOD detection

The DINO network structure  $g(x)$  used in this work consists of a ViT-S as backbone, which maps the input  $x$  to a  $d$ -dimensional feature vector  $f \in \mathbb{R}^d$ , and two fully connected



Table 2. AUROC scores for OOD Detection with CIFAR10 as  $\mathcal{D}_{train}^{in}$  and different  $\mathcal{D}_{neg}$ . ImgN denotes ImageNet samples.

| Negative Sampling:         |                            | None          | Auxiliary |              |         |       |         |        |              |       | In-Dist      |
|----------------------------|----------------------------|---------------|-----------|--------------|---------|-------|---------|--------|--------------|-------|--------------|
| $\mathcal{D}_{train}^{in}$ | $\mathcal{D}_{test}^{out}$ | DINO          | ImgN      | Rot.         | Rot.360 | DTI   | Perm-16 | Perm-4 | Rot.         | Pix.  | Rot.         |
|                            |                            | $\lambda = 0$ |           | ImgN         | ImgN    |       | ImgN    | ImgN   | DTI          | Perm. | In-Dist.     |
| CIFAR10                    | CIFAR100                   | 90.29         | 90.46     | 92.51        | 88.62   | 93.77 | 88.32   | 89.57  | 93.77        | 87.67 | <b>93.96</b> |
|                            | SVHN                       | 99.38         | 99.50     | 99.69        | 99.42   | 99.86 | 99.59   | 99.13  | 99.86        | 99.62 | <b>99.92</b> |
|                            | ImageNet30                 | 88.81         | 89.96     | 94.16        | 88.95   | 93.39 | 89.17   | 84.71  | <b>96.04</b> | 87.46 | 91.69        |
|                            | TinyImageNet               | 91.07         | 94.14     | <b>96.28</b> | 91.60   | 94.53 | 89.72   | 91.27  | 95.64        | 89.39 | 94.27        |
|                            | LSUN                       | 92.20         | 93.41     | 98.08        | 93.24   | 98.56 | 94.58   | 89.32  | <b>99.12</b> | 93.33 | 94.93        |
|                            | STL10                      | 66.50         | 77.65     | 77.29        | 72.41   | 72.01 | 69.22   | 68.81  | <b>81.49</b> | 68.55 | 69.11        |
|                            | Places365                  | 91.28         | 93.12     | 97.14        | 92.58   | 97.03 | 92.77   | 87.63  | <b>98.12</b> | 91.89 | 93.53        |
|                            | Texture                    | 96.21         | 95.01     | <b>99.16</b> | 93.93   | 97.55 | 93.38   | 89.86  | 95.11        | 93.08 | 98.29        |
|                            | Average                    | 89.47         | 91.66     | 94.29        | 90.09   | 93.34 | 89.59   | 87.54  | <b>94.89</b> | 88.87 | 91.96        |

layers as head, which converts the features vector  $f$  to a  $K$ -dimensional output vector that enters the softmax layer. We define an anomaly detection score,  $\mathcal{S}$ , for the OOD test data  $\mathcal{D}_{test}^{out}$  by computing the cosine similarity between the feature vector for a test image  $f_{test}$  and all features vectors  $f_m$  of the in-distribution training set. Instead of taking the maximum cosine similarity as a OOD score, we opt for a temperature weighted non-linear score,

$$\mathcal{S}(x) = -\frac{1}{M} \sum_{m=1}^M \exp\left(\frac{1}{\tau} \cdot \frac{f_{test}^T f_m}{\|f_{test}\| \|f_m\|}\right), \quad (6)$$

with  $\tau = 0.04$  a fixed temperature and  $M$  the number of in-distribution training samples. The score is used to evaluate OOD performance by reporting the Area Under the Receiver Operating characteristic Curve (AUROC) between a given OOD test set and the in-distribution test set.

### 4.3. Experimental results

In Tab. 1, quantitative results are reported for CIFAR10 and CIFAR100 as in-distribution. We report results with ImageNet rotated samples as well as combining them with in-distribution rotated samples (Combined). When using CIFAR10 as  $\mathcal{D}_{train}^{in}$ , the proposed method shows superior performance in 6 out of 8 (75%) OOD datasets compared to current SOTA self-supervised methods. Surprisingly, we even surpass hybrid methods, where self-supervised training is combined with human-labelled images. By further leveraging in-distribution negatives, we are able to surpass all other methods in CIFAR100 by 3.57% and 0.96% against self-supervised and supervised methods, respectively. Therefore, we believe that near OOD performance can have a significant improvement when there is prior knowledge in terms of choosing the appropriate dataset-specific transformation to form good negative examples, applied on  $\mathcal{D}_{train}^{in}$ , such as rotating CIFAR10 images.

Our results are roughly consistent for CIFAR100 as  $\mathcal{D}_{train}^{in}$ . Again, we report superior performance in 6 out of 8 (75%). Far OOD datasets have a substantial benefit, such as LSUN where we report a 5.53% gain against the best self-supervised method. Still, our results on near OOD on CIFAR10 are on par with self-supervised methods [46], while still lacking behind supervised methods. As illustrated in Tab. 1, there was no gain in near OOD when adding rotated in-distribution samples, which is justified by the fact that the provided rotations do not form as good negative samples as in CIFAR10. Our findings on the chosen shifting transformations are in line with [33], wherein translation is considered to be the best choice for CIFAR100.

In Tab. 2, we investigate several ways to generate negative samples, as detailed in Sec. 4.1. It can be observed that by rotating both ImageNet and DTI with  $R$ , both distributions demonstrate an average performance gain of 2.63% and 1.55% respectively compared to no additional transformation. On the contrary, when applying the Rot.360 transformation on ImageNet, performance deteriorates by 1.57% on average. Rotated ImageNet and DTI reached the highest gains of 10.79% and 14.99% in STL10 compared to DINO. We claim that leveraging auxiliary rotated datasets best suits cases when there is a big class overlap, such as CIFAR10 and STL10. Interestingly, rotated CIFAR10 samples outperform all other strategies in near OOD (CIFAR100). This finding further confirms that dataset-specific shifting transformations can form good near OOD boundaries when treated as negative examples. Apart from OOD detection in CIFAR100, Rot. In-Dist still shows inferior results compared to Rot. ImageNet and Rot. DTI.

It is worth noting that we abstain from reporting the performance of DTI in Tab. 1, since labels were used to form this subset of 300K images. Nonetheless, we show that the introduced method is not specifically linked to ImageNet, but only assumes that a broad distribution of unlabelled data

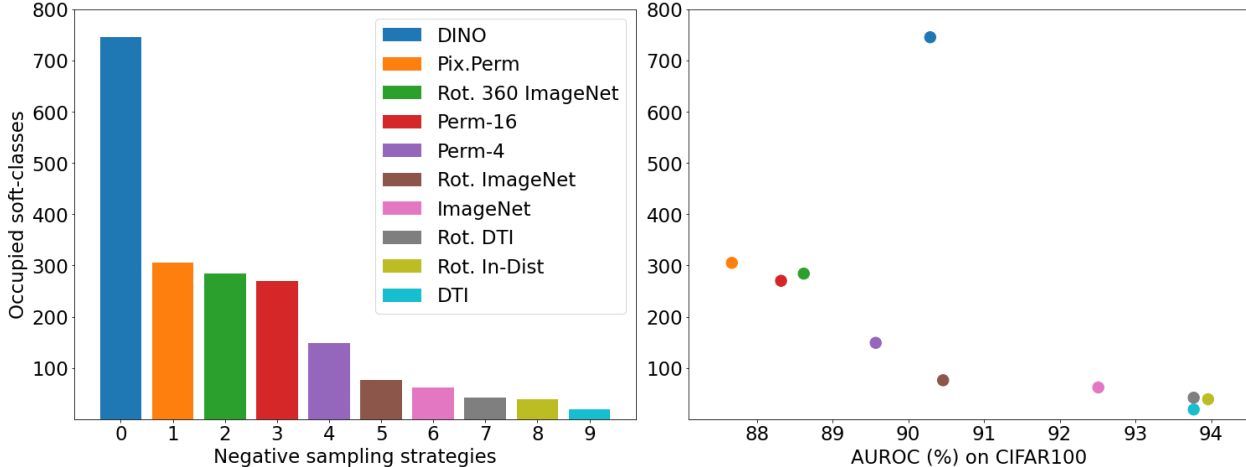


Figure 2. We define a soft-class as “occupied” if the probability assigned to that soft-class is greater than the average probability of all  $K$  soft-classes. Colors indicate multiple  $\mathcal{D}_{neg}$  and are shared within the two plots. The teacher network  $g_t$  is used to generate  $p_t$  from  $\mathcal{D}_{test}^{in}$ . Training is performed on CIFAR10. **Left:**  $\mathcal{D}_{test}^{in}$  occupy less soft-classes with negative sampling compared to the DINO baseline. **Right:** relationship of occupied soft-classes with respect to AUROC score in CIFAR100.

is available. On top of that, the reported results indicate that one can use fewer image samples than ImageNet. Finally, we report an inferior (or on par) average AUROC score when employing Pix. Perm, Perm-4, and Perm-16 against the vanilla DINO method using ImageNet as the auxiliary dataset.

## 5. Discussion

**Do negative samples lead to more condensed in-distribution representations?** To understand the impact of the introduced negative sampling methods, we investigate how many of the  $K = 4096$  soft-classes are “occupied” by the  $\mathcal{D}_{test}^{in}$  after training on CIFAR10. A soft-class is considered occupied if the probability assigned to that soft-class from all test data is greater than the average soft-class probability. As depicted in Fig. 2 (left), negative sampling reduces the occupied classes compared to the DINO baseline. This observation is independent of how  $\mathcal{D}_{neg}$  is created. More specifically, Rot. ImageNet, Rot. DTI, and Rot. In-Dist use roughly the same number of soft-classes and achieve SOTA AUROC scores on CIFAR100. By combining the aforementioned qualitative evaluations with Tab. 2, we claim that by contrasting  $\mathcal{D}_{train}^{in}$  against  $\mathcal{D}_{neg}$  a more condensed representation can be learnt.

By incorporating additional transformations, the negative samples become more dissimilar to  $\mathcal{D}_{train}^{in}$ , which renders the representations to be even more condensed. Besides, the transformations  $\mathcal{T}$  applied on  $\mathcal{D}_{train}^{in}$  (i.e. crops, jitter) are keeping  $\mathcal{D}_{train}^{in}$  and  $\mathcal{D}_{test}^{in}$  close together. This finding is considered a promising research direction for future work.

In addition, a relationship between AUROC scores on CIFAR10 against CIFAR100 and the occupied classes is highlighted in Fig. 2 (right). In particular, negative sampling strategies can be evaluated by looking at  $\mathcal{D}_{test}^{in}$ . Nonetheless, we note that this correlation becomes weaker when comparing average AUROC percentages across all considered datasets, especially when the negative sampling strategy performs worse than the baseline.

**Is OOD detection related to in-distribution classification?** To answer this question, we investigate if there is a relationship between the OOD detection performance and the K-NN accuracy, determined from human-generated labels. To do so, we use CIFAR10 as  $\mathcal{D}_{train}^{in}$  and CIFAR100 and Texture as  $\mathcal{D}_{test}^{out}$ , as representative cases of near OOD and far OOD respectively. We find that the OOD AUROC score is positively correlated with K-NN accuracy for both near and far OOD detection (Fig. 3, top row).

**How to choose good negative examples?** Ideally, the distribution of negative examples,  $\mathcal{D}_{neg}$ , should share most of the features’ statistics of the in-distribution,  $\mathcal{D}^{in}$ , but discrimination between negative examples and in-distribution examples should be possible in practice, e.g. by a deep neural network. The statistical closeness between  $\mathcal{D}_{neg}$  and  $\mathcal{D}^{in}$  is necessary to ensure high detection performance for near OOD examples. In practice, the design of  $\mathcal{D}_{neg}$  is difficult in absence of labels and some domain knowledge is needed to avoid significant overlap with the in-distribution. In this work, we apply rotation to images of natural objects to reduce the overlap with the in-distribution.

To quantify the statistical relatedness we apply our OOD score (Eq. (6)) to a test set of in-distribution ex-

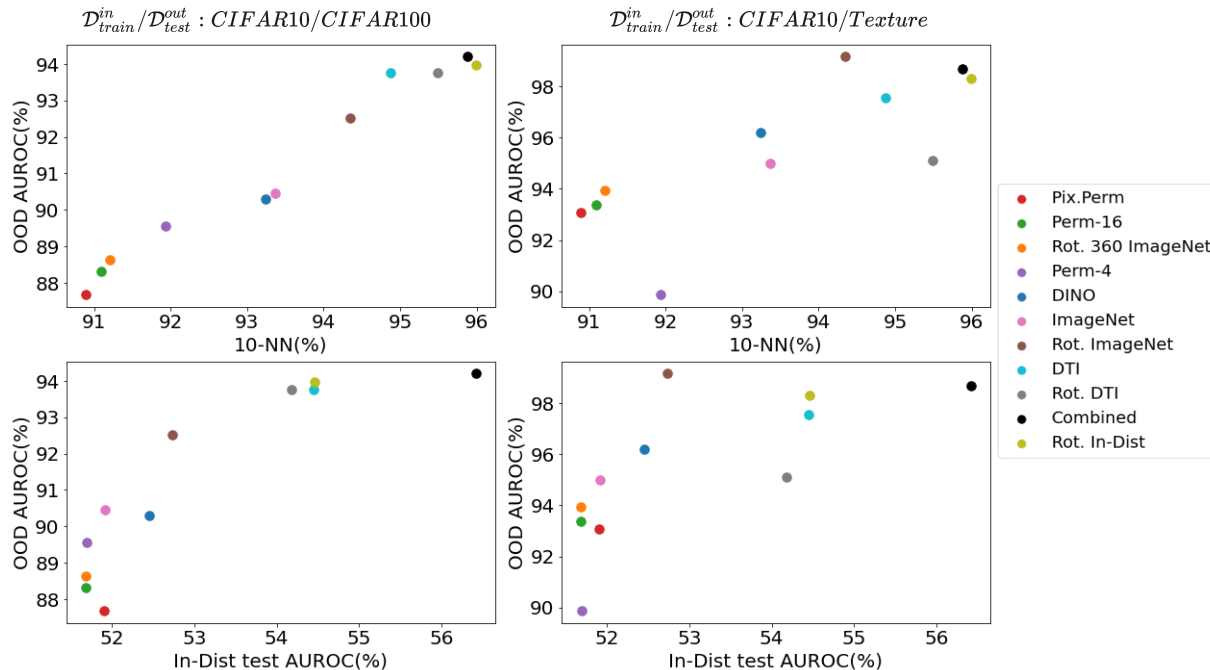


Figure 3. We evaluate different models trained on CIFAR10 for two OOD datasets, CIFAR100 (left column) and Texture (right column). In each plot, points indicate different negative sampling strategies (colors are shared). **Top row**: correlation between OOD detection AUROC and K-NN accuracy on  $\mathcal{D}_{test}^{in}$ . **Bottom row**: correlation between OOD detection AUROC and AUROC score of  $\mathcal{D}_{train}^{in}$  vs.  $\mathcal{D}_{test}^{in}$ . We observe models with higher sensitivity to detect  $\mathcal{D}_{test}^{in}$  as outliers have higher OOD detection performance.

amples. The degree of rejection of in-distribution examples gives us a measure about the sensitivity of the OOD score to examples that have very similar features statistics to  $\mathcal{D}_{train}^{in}$ . Based on this measure, we find that the combination of rotated ImageNet examples and rotated in-distribution examples (“Combined”) generates the statistically closest negative examples for CIFAR10 among all the  $D_{neg}$  we used in experiments (Fig. 3). This result is confirmed in Tab. 1 and Tab. 2, where the near OOD detection problem CIFAR10/CIFAR100 receives the highest AUROC score for “Combined”. However, using “Combined” as  $D_{neg}$  is not the best option for the semantically far OOD detection problem CIFAR10/Texture (Tab. 2). This can be explained by the resulting insensitivity of the OOD score to all the low-level features shared between the in-distribution and rotated in-distribution that may help to reject Texture examples as OOD. In this case, taking rotated ImageNet examples as negatives is a better option.

## 6. Conclusion

In this work, we presented a new general method for self-supervised OOD detection. We demonstrated how self-distillation can be extended to account for positive and negative examples by introducing an auxiliary objective.

The proposed objective introduces a form of contrastive learning, which pushes negative samples to be uniformly distributed among the existing in-distribution soft-classes. Additionally, we thoroughly studied how negative samples can be generated by comparing multiple variations, based on two auxiliary datasets. The different negative sampling approaches were compared in terms of OOD detection performance, as well as in terms of their impact on the in-distribution classification. Insights regarding choosing transformations with respect to near and far OOD were provided. The proposed method outperforms current SOTA for self-supervised OOD detection methods in the majority of OOD benchmark datasets for both CIFAR10 and CIFAR100 as  $\mathcal{D}_{train}^{in}$ . We hope that the provided insights of our analysis will shed light on how to choose negative samples in more challenging vision domains.

## References

- [1] Jinwon An and Sungzoon Cho. Variational autoencoder based anomaly detection using reconstruction probability. 2015. 3
- [2] Liron Bergman and Yedid Hoshen. Classification-based anomaly detection for general data. In *8th International Conference on Learning Representations, ICLR 2020, Addis*



- Ababa, Ethiopia, April 26-30, 2020. OpenReview.net, 2020. 3
- [3] Mathilde Caron, Ishan Misra, Julien Mairal, Priya Goyal, Piotr Bojanowski, and Armand Joulin. Unsupervised learning of visual features by contrasting cluster assignments. *arXiv preprint arXiv:2006.09882*, 2020. 2, 4
- [4] Mathilde Caron, Hugo Touvron, Ishan Misra, Hervé Jégou, Julien Mairal, Piotr Bojanowski, and Armand Joulin. Emerging properties in self-supervised vision transformers. *arXiv preprint arXiv:2104.14294*, 2021. 2, 4, 5
- [5] Ting Chen, Simon Kornblith, Mohammad Norouzi, and Geoffrey Hinton. A simple framework for contrastive learning of visual representations. In *International conference on machine learning*, pages 1597–1607. PMLR, 2020. 2, 4
- [6] Hyunsoo Cho, Jinseok Seol, and Sang-goo Lee. Masked contrastive learning for anomaly detection. In Zhi-Hua Zhou, editor, *Proceedings of the Thirtieth International Joint Conference on Artificial Intelligence, IJCAI 2021, Virtual Event / Montreal, Canada, 19-27 August 2021*, pages 1434–1441. ijcai.org, 2021. 3
- [7] Sung-Ik Choi and Sae-Young Chung. Novelty detection via blurring. In *8th International Conference on Learning Representations, ICLR 2020, Addis Ababa, Ethiopia, April 26-30, 2020*. OpenReview.net, 2020. 3
- [8] Ching-Yao Chuang, Joshua Robinson, Yen-Chen Lin, Antonio Torralba, and Stefanie Jegelka. Debaised contrastive learning. In Hugo Larochelle, Marc’Aurelio Ranzato, Raia Hadsell, Maria-Florina Balcan, and Hsuan-Tien Lin, editors, *Advances in Neural Information Processing Systems 33: Annual Conference on Neural Information Processing Systems 2020, NeurIPS 2020, December 6-12, 2020, virtual*, 2020. 3
- [9] Mircea Cimpoi, Subhansu Maji, Iasonas Kokkinos, Sammy Mohamed, and Andrea Vedaldi. Describing textures in the wild. *CoRR*, abs/1311.3618, 2013. 5
- [10] Adam Coates, Andrew Ng, and Honglak Lee. An analysis of single-layer networks in unsupervised feature learning. In Geoffrey Gordon, David Dunson, and Miroslav Dudík, editors, *Proceedings of the Fourteenth International Conference on Artificial Intelligence and Statistics*, volume 15 of *Proceedings of Machine Learning Research*, pages 215–223. Fort Lauderdale, FL, USA, 11–13 Apr 2011. PMLR. 1
- [11] Terrance DeVries and Graham W. Taylor. Learning confidence for out-of-distribution detection in neural networks. *CoRR*, abs/1802.04865, 2018. 2
- [12] Alexey Dosovitskiy, Lucas Beyer, Alexander Kolesnikov, Dirk Weissenborn, Xiaohua Zhai, Thomas Unterthiner, Mostafa Dehghani, Matthias Minderer, Georg Heigold, Sylvain Gelly, Jakob Uszkoreit, and Neil Houlsby. An image is worth 16x16 words: Transformers for image recognition at scale. In *International Conference on Learning Representations*, 2021. 2
- [13] Alexey Dosovitskiy, Philipp Fischer, Jost Tobias Springenberg, Martin A. Riedmiller, and Thomas Brox. Discriminative unsupervised feature learning with exemplar convolutional neural networks. *IEEE Trans. Pattern Anal. Mach. Intell.*, 38(9):1734–1747, 2016. 3
- [14] Stanislav Fort, Jie Ren, and Balaji Lakshminarayanan. Exploring the limits of out-of-distribution detection. *ArXiv*, abs/2106.03004, 2021. 1, 2
- [15] Stanislav Fort, Jie Ren, and Balaji Lakshminarayanan. Exploring the limits of out-of-distribution detection. *arXiv preprint arXiv:2106.03004*, 2021. 2, 3
- [16] Izhak Golan and Ran El-Yaniv. Deep anomaly detection using geometric transformations. In Samy Bengio, Hanna M. Wallach, Hugo Larochelle, Kristen Grauman, Nicolò Cesa-Bianchi, and Roman Garnett, editors, *Advances in Neural Information Processing Systems 31: Annual Conference on Neural Information Processing Systems 2018, NeurIPS 2018, December 3-8, 2018, Montréal, Canada*, pages 9781–9791, 2018. 3
- [17] Jean-Bastien Grill, Florian Strub, Florent Altché, Corentin Tallec, Pierre Richemond, Elena Buchatskaya, Carl Doersch, Bernardo Avila Pires, Zhaohan Guo, Mohammad Gheshlaghi Azar, Bilal Piot, koray kavukcuoglu, Remi Munos, and Michal Valko. Bootstrap your own latent - a new approach to self-supervised learning. In H. Larochelle, M. Ranzato, R. Hadsell, M. F. Balcan, and H. Lin, editors, *Advances in Neural Information Processing Systems*, volume 33, pages 21271–21284. Curran Associates, Inc., 2020. 5
- [18] Kaiming He, Haoqi Fan, Yuxin Wu, Saining Xie, and Ross Girshick. Momentum contrast for unsupervised visual representation learning. In *Proceedings of the IEEE/CVF Conference on Computer Vision and Pattern Recognition*, pages 9729–9738, 2020. 2
- [19] Matthias Hein, Maksym Andriushchenko, and Julian Bitterwolf. Why relu networks yield high-confidence predictions far away from the training data and how to mitigate the problem. 2019. 1
- [20] Dan Hendrycks and Kevin Gimpel. A baseline for detecting misclassified and out-of-distribution examples in neural networks. In *5th International Conference on Learning Representations, ICLR 2017, Toulon, France, April 24-26, 2017, Conference Track Proceedings*. OpenReview.net, 2017. 2
- [21] Dan Hendrycks, Xiaoyuan Liu, Eric Wallace, Adam Dziedziec, Rishabh Krishnan, and Dawn Song. Pretrained transformers improve out-of-distribution robustness. In Dan Jurafsky, Joyce Chai, Natalie Schluter, and Joel R. Tetreault, editors, *Proceedings of the 58th Annual Meeting of the Association for Computational Linguistics, ACL 2020, Online, July 5-10, 2020*, pages 2744–2751. Association for Computational Linguistics, 2020. 3
- [22] Dan Hendrycks, Mantas Mazeika, and Thomas G. Dietterich. Deep anomaly detection with outlier exposure. In *7th International Conference on Learning Representations, ICLR 2019, New Orleans, LA, USA, May 6-9, 2019*. OpenReview.net, 2019. 2, 3, 5
- [23] Dan Hendrycks, Mantas Mazeika, Saurav Kadavath, and Dawn Song. Using self-supervised learning can improve model robustness and uncertainty. In Hanna M. Wallach, Hugo Larochelle, Alina Beygelzimer, Florence d’Alché-Buc, Emily B. Fox, and Roman Garnett, editors, *Advances in Neural Information Processing Systems 32: Annual Conference on Neural Information Processing Systems*

- 2019, *NeurIPS 2019, December 8-14, 2019, Vancouver, BC, Canada*, pages 15637–15648, 2019. 2, 3, 5
- [24] Prannay Khosla, Piotr Teterwak, Chen Wang, Aaron Sarna, Yonglong Tian, Phillip Isola, Aaron Maschinot, Ce Liu, and Dilip Krishnan. Supervised contrastive learning. *arXiv preprint arXiv:2004.11362*, 2020. 3
- [25] Diederik P. Kingma and Max Welling. Auto-encoding variational bayes. In Yoshua Bengio and Yann LeCun, editors, *2nd International Conference on Learning Representations, ICLR 2014, Banff, AB, Canada, April 14-16, 2014, Conference Track Proceedings*, 2014. 1, 3
- [26] Rajat Koner, Poulami Sinhamahapatra, Karsten Roscher, Stephan Günnemann, and Volker Tresp. Oodformer: Out-of-distribution detection transformer. *CoRR*, abs/2107.08976, 2021. 3
- [27] Alex Krizhevsky, Geoffrey Hinton, et al. Learning multiple layers of features from tiny images. 2009. 1
- [28] Kimin Lee, Honglak Lee, Kibok Lee, and Jinwoo Shin. Training confidence-calibrated classifiers for detecting out-of-distribution samples. In *6th International Conference on Learning Representations, ICLR 2018, Vancouver, BC, Canada, April 30 - May 3, 2018, Conference Track Proceedings*. OpenReview.net, 2018. 2, 3
- [29] Shiyu Liang, Yixuan Li, and R. Srikant. Enhancing the reliability of out-of-distribution image detection in neural networks. In *6th International Conference on Learning Representations, ICLR 2018, Vancouver, BC, Canada, April 30 - May 3, 2018, Conference Track Proceedings*. OpenReview.net, 2018. 2
- [30] Ilya Loshchilov and Frank Hutter. Fixing weight decay regularization in adam. 2018. 5
- [31] Marc Masana, Idoia Ruiz, Joan Serrat, Joost van de Weijer, and Antonio M. López. Metric learning for novelty and anomaly detection. In *British Machine Vision Conference 2018, BMVC 2018, Newcastle, UK, September 3-6, 2018*, page 64. BMVA Press, 2018. 3
- [32] Sina Mohseni, Mandar Pitale, J. B. S. Yadawa, and Zhangyang Wang. Self-supervised learning for generalizable out-of-distribution detection. In *The Thirty-Fourth AAAI Conference on Artificial Intelligence, AAAI 2020, The Thirty-Second Innovative Applications of Artificial Intelligence Conference, IAAI 2020, The Tenth AAAI Symposium on Educational Advances in Artificial Intelligence, EAAI 2020, New York, NY, USA, February 7-12, 2020*, pages 5216–5223. AAAI Press, 2020. 2
- [33] Sina Mohseni, Arash Vahdat, and Jay Yadawa. Shifting transformation learning for out-of-distribution detection, 2021. 2, 3, 5, 6
- [34] Eric Nalisnick, Akihiro Matsukawa, Yee Whye Teh, Dilan Gorur, and Balaji Lakshminarayanan. Do deep generative models know what they don’t know?, 2019. 1, 3
- [35] Eric T. Nalisnick, Akihiro Matsukawa, Yee Whye Teh, and Balaji Lakshminarayanan. Detecting out-of-distribution inputs to deep generative models using a test for typicality. *CoRR*, abs/1906.02994, 2019. 3
- [36] Yuval Netzer, Tiejie Wang, Adam Coates, A. Bissacco, Bo Wu, and A. Ng. Reading digits in natural images with unsupervised feature learning. 2011. 5
- [37] Anh Nguyen, Jason Yosinski, and Jeff Clune. Deep neural networks are easily fooled: High confidence predictions for unrecognizable images. In *2015 IEEE Conference on Computer Vision and Pattern Recognition (CVPR)*, pages 427–436, 2015. 1
- [38] Stanislav Pidhorskyi, Ranya Almohsen, and Gianfranco Doretto. Generative probabilistic novelty detection with adversarial autoencoders. In Samy Bengio, Hanna M. Wallach, Hugo Larochelle, Kristen Grauman, Nicolò Cesa-Bianchi, and Roman Garnett, editors, *Advances in Neural Information Processing Systems 31: Annual Conference on Neural Information Processing Systems 2018, NeurIPS 2018, December 3-8, 2018, Montréal, Canada*, pages 6823–6834, 2018. 3
- [39] Jie Ren, Peter J. Liu, Emily Fertig, Jasper Snoek, Ryan Poplin, Mark A. DePristo, Joshua V. Dillon, and Balaji Lakshminarayanan. Likelihood ratios for out-of-distribution detection. In Hanna M. Wallach, Hugo Larochelle, Alina Beygelzimer, Florence d’Alché-Buc, Emily B. Fox, and Roman Garnett, editors, *Advances in Neural Information Processing Systems 32: Annual Conference on Neural Information Processing Systems 2019, NeurIPS 2019, December 8-14, 2019, Vancouver, BC, Canada*, pages 14680–14691, 2019. 3
- [40] Danilo Jimenez Rezende and Shakir Mohamed. Variational inference with normalizing flows, 2016. 1
- [41] Olga Russakovsky, Jia Deng, Hao Su, Jonathan Krause, Sanjeev Satheesh, Sean Ma, Zhiheng Huang, Andrej Karpathy, Aditya Khosla, Michael Bernstein, et al. Imagenet large scale visual recognition challenge. *International journal of computer vision*, 115(3):211–252, 2015. 2, 5
- [42] Robin Schirrmester, Yuxuan Zhou, Tonio Ball, and Dan Zhang. Understanding anomaly detection with deep invertible networks through hierarchies of distributions and features. In Hugo Larochelle, Marc’Aurelio Ranzato, Raia Hadsell, Maria-Florina Balcan, and Hsuan-Tien Lin, editors, *Advances in Neural Information Processing Systems 33: Annual Conference on Neural Information Processing Systems 2020, NeurIPS 2020, December 6-12, 2020, virtual*, 2020. 3
- [43] Vikash Sehwal, Mung Chiang, and Prateek Mittal. Ssd: A unified framework for self-supervised outlier detection. In *International Conference on Learning Representations*, 2021. 2, 3, 5
- [44] Joan Serra, David Álvarez, Vicenç Gómez, Olga Slizovskaia, José F. Núñez, and Jordi Luque. Input complexity and out-of-distribution detection with likelihood-based generative models. In *8th International Conference on Learning Representations, ICLR 2020, Addis Ababa, Ethiopia, April 26-30, 2020*. OpenReview.net, 2020. 3
- [45] Gabi Shalev, Yossi Adi, and Joseph Keshet. Out-of-distribution detection using multiple semantic label representations. In Samy Bengio, Hanna M. Wallach, Hugo Larochelle, Kristen Grauman, Nicolò Cesa-Bianchi, and Roman Garnett, editors, *Advances in Neural Information Processing Systems 31: Annual Conference on Neural Information Processing Systems 2018, NeurIPS 2018, December 3-8, 2018, Montréal, Canada*, pages 7386–7396, 2018. 3
- [46] Jihoon Tack, Sangwoo Mo, Jongheon Jeong, and Jinwoo Shin. Csi: Novelty detection via contrastive learning on dis-

- tributionally shifted instances. In *34th Conference on Neural Information Processing Systems (NeurIPS) 2020*, volume 33, pages 11839–11852, 2020. [2](#), [3](#), [4](#), [5](#), [6](#)
- [47] Antonio Torralba, Rob Fergus, and William T Freeman. 80 million tiny images: A large data set for nonparametric object and scene recognition. *IEEE transactions on pattern analysis and machine intelligence*, 30(11):1958–1970, 2008. [5](#)
- [48] Aäron van den Oord, Nal Kalchbrenner, and Koray Kavukcuoglu. Pixel recurrent neural networks. In Maria-Florina Balcan and Kilian Q. Weinberger, editors, *Proceedings of the 33rd International Conference on Machine Learning, ICML 2016, New York City, NY, USA, June 19-24, 2016*, volume 48 of *JMLR Workshop and Conference Proceedings*, pages 1747–1756. JMLR.org, 2016. [1](#)
- [49] Ashish Vaswani, Noam Shazeer, Niki Parmar, Jakob Uszkoreit, Llion Jones, Aidan N Gomez, Łukasz Kaiser, and Illia Polosukhin. Attention is all you need. In *Advances in neural information processing systems*, pages 5998–6008, 2017. [3](#)
- [50] Apoorv Vyas, Nataraj Jammalamadaka, Xia Zhu, Dipankar Das, Bharat Kaul, and Theodore L. Willke. Out-of-distribution detection using an ensemble of self supervised leave-out classifiers. In Vittorio Ferrari, Martial Hebert, Cristian Sminchisescu, and Yair Weiss, editors, *Computer Vision - ECCV 2018 - 15th European Conference, Munich, Germany, September 8-14, 2018, Proceedings, Part VIII*, volume 11212 of *Lecture Notes in Computer Science*, pages 560–574. Springer, 2018. [2](#)
- [51] Jim Winkens, Rudy Bunel, Abhijit Guha Roy, Robert Stanforth, Vivek Natarajan, Joseph R. Ledsam, Patricia MacWilliams, Pushmeet Kohli, Alan Karthikesalingam, Simon Kohl, A. Taylan Cemgil, S. M. Ali Eslami, and Olaf Ronneberger. Contrastive training for improved out-of-distribution detection. *CoRR*, abs/2007.05566, 2020. [1](#), [2](#)
- [52] Jim Winkens, Rudy Bunel, Abhijit Guha Roy, Robert Stanforth, Vivek Natarajan, Joseph R. Ledsam, Patricia MacWilliams, Pushmeet Kohli, Alan Karthikesalingam, Simon Kohl, A. Taylan Cemgil, S. M. Ali Eslami, and Olaf Ronneberger. Contrastive training for improved out-of-distribution detection. *CoRR*, abs/2007.05566, 2020. [3](#)
- [53] Zhisheng Xiao, Qing Yan, and Yali Amit. Likelihood regret: An out-of-distribution detection score for variational auto-encoder. In Hugo Larochelle, Marc’Aurelio Ranzato, Raia Hadsell, Maria-Florina Balcan, and Hsuan-Tien Lin, editors, *Advances in Neural Information Processing Systems 33: Annual Conference on Neural Information Processing Systems 2020, NeurIPS 2020, December 6-12, 2020, virtual*, 2020. [3](#)
- [54] E Xie, W Wang, Z Yu, A Anandkumar, JM Alvarez, and P Luo. Segformer: Simple and efficient design for semantic segmentation with transformers. arxiv 2021. *arXiv preprint arXiv:2105.15203*. [2](#)
- [55] Fisher Yu, Yinda Zhang, Shuran Song, Ari Seff, and Jianxiong Xiao. LSUN: construction of a large-scale image dataset using deep learning with humans in the loop. *CoRR*, abs/1506.03365, 2015. [5](#)
- [56] Hongjie Zhang, Ang Li, Jie Guo, and Yanwen Guo. Hybrid models for open set recognition. In Andrea Vedaldi, Horst Bischof, Thomas Brox, and Jan-Michael Frahm, editors, *Computer Vision - ECCV 2020 - 16th European Conference, Glasgow, UK, August 23-28, 2020, Proceedings, Part III*, volume 12348 of *Lecture Notes in Computer Science*, pages 102–117. Springer, 2020. [3](#)
- [57] Bolei Zhou, Agata Lapedriza, Aditya Khosla, Aude Oliva, and Antonio Torralba. Places: A 10 million image database for scene recognition. *IEEE Transactions on Pattern Analysis and Machine Intelligence*, 40(6):1452–1464, 2018. [5](#)
- [58] Bo Zong, Qi Song, Martin Renqiang Min, Wei Cheng, Cristian Lumezanu, Dae-ki Cho, and Haifeng Chen. Deep autoencoding gaussian mixture model for unsupervised anomaly detection. In *6th International Conference on Learning Representations, ICLR 2018, Vancouver, BC, Canada, April 30 - May 3, 2018, Conference Track Proceedings*. OpenReview.net, 2018. [3](#)